CHAPTER-2

LITERATURE REVIEW

2.1 Groundwater contamination

A change in physical, chemical or biological properties of the groundwater used for drinking purpose may lead to negative impacts on human health. The contamination of the groundwater is generally irreversible i.e., once it is contaminated; it is difficult to restore the aquifer to its original water quality. Nitrate, fluoride and arsenic are the common anions that may be responsible for groundwater contamination. Many such groundwater sources suffer from these contaminants. A brief description of forms, origin and their health effects is presented in Table 2.1.

Table 2.1: Common groundwater contaminants

Contaminants	Species	Origin	Health affect
Nitrate	Nitrate (NO_3^-), Nitrite (NO_2^-), Nitrogen (N_2)	Nitrogen fixation, Chemical fertilizers and Animal manure	Methaemoglobinemia, Gastric cancer
Fluoride	Fluoride (F^-), Hydrogen Fluoride (HF)	Fluorspar, Cryolite, Fluorite and Fluorapatite	Nausea, Salivation, Vomiting, Diarrhoea and Abdominal Pain, Emaciation, Stiffness of joints and Abnormal teeth and bones
Arsenic	Arsenite (As(III)) are H_3AsO_3, $H_2AsO_3^-$, $HAsO_3^{2-}$, AsO_3^{3-} Arsenate (As(V)) are H_3AsO_4, $H_2AsO_4^-$, $HAsO_4^{2-}$, AsO_4^{3-}	Geological realgar (As_2S_2), Orpiment (As_2S_3) and Iron pyrites (geogenic) and Anthropogenic (human activities)	Vomiting, Diarrhea, Kidney, Liver and Lung problems

(Source: CGWB, 2014; 2018)

The presence of nitrate, fluoride or arsenic in the drinking water beyond permissible limits require their treatment before use. Several methods and approaches have been developed and evaluated. Different methods have their own merits and limitations with respect to their operating conditions, such as optimal pH, temperature, efficiency, operating costs and their disposal. The main technologies for removing such contaminants include ion exchange, coagulation, membrane filtration, and adsorption (Patel et al., 2019). Table 2.2 provides a general summary of their performance in terms of different operational conditions, removal efficiency, relative cost, and post-treatment requirements.

Table 2.2 Comparative analyses of the removal technologies applicable for anionic contaminants removal from water

Technologies	Operational parameter and efficiency					
	pH and Temperature	**Post-treatment**	**Removal efficiency**	**Operational cost**	**Disposal**	**Reference**
Ion Exchange	Not important	Required due to corrosivity of product water	60-90%	Medium	Waste brine	Onyango et al., 2005; 2006 Khoei et al., 2019
Coagulation Precipitation	Important	Required due to the production of by-products	60-70%	High	No waste	Stephenson et al., 1996; Randtke S.J., 1988; Patel et al., 2019
Membrane Process	Not important	Required due to corrosivity of product water	80-95%	High	High total dissolved solids (TDS)	Madaeni et al., 1999; Pendergast et al., 2011
Adsorption	Important	Often not required	Varies with adsorbents	Medium	Saturated/spent adsorbent	Ali et al., 2006; Faust et al., 2013; Xie et al., 2018

(Source: Patel et al., 2019)

Removal of anionic contaminants from water is a challenge and is very important from public health point of view. The most prevalent anionic contaminants in groundwater include nitrate, fluoride and arsenic. Arsenic has received a lot of attention from researchers. An extensive literature search was carried out on nitrate, fluoride and arsenic removal. Although all three selected contaminants (nitrate, fluoride and arsenic) are anionic in nature, many of their behaviors are unique and uncommon. Therefore, it is important to review various options for their removal from the aqueous environment.

2.2 Technologies for nitrate removal from water

There are two options to reduce the high concentration of nitrate in drinking water. The first is blending with fresh water with low nitrate concentration, or change the source of water. Use of treatment processes such as ion exchange, adsorption, reverse osmosis, biological denitrification and chemical reduction, etc. are the second alternative to achieve the safe limit for nitrate. The most important thing about these removal methods, however, is that none of them remove nitrate completely. The treatment method may remove nitrate partially with varying degrees of efficiency, much of which may depend on other substances found in the water (Bhatnagar et al., 2011). Green and Shelef (1994); Kapoor and Virarghavan (1997); Shrimali and Singh (2001) have published some of the excellent reviews on nitrate removal from drinking water. The ion exchange process is more suitable for nitrate removal from groundwater, while biological denitrification is more suitable for surface water (Kapoor and Virarghavan, 1997). Many studies, such as Samatya et al., (2006), Chabani et al., (2006), Chabani et al., (2009), Milmile et al., (2011) have given details on ion exchange

process. The adsorption process is considered to be the most attractive method of nitrate removal in terms of cost, simplicity of design and operation (Bhatnagar et al., 2010). Some of the other methods include chemical denitrification (Huang and Zhang, 2004; Chen et al., 2005; Liou et al., 2005; Kumar and Chakraborty, 2006; Ahn et al., 2008), reverse osmosis (Schoeman and Steyn, 2003), electrodialysis (Hell et al., 1998) , catalytic denitrification (Pintar et al., 2001; Barrabes and Sa, 2011; Hasnat et al., 2009, Hasnat et al., 2012; Healy et al., 2012), electrocoagulation (Kumar and Goel, 2010), electrochemical (He et al., 2019) and biological denitrification (Healy et al., 2012; Cameron and Schipper, 2012; Zhao et al., 2012). Some of the other references on nitrate removal from water are Bhatnagar and Sillanpa (2011), Christianson et al. (2013; 2015), Mohsenipour et al. (2015), Mahdavi et al. (2018), and Patel et al. (2019).

For small-scale applications, however, treatment methods based on adsorption, ion exchange, and reverse osmosis are most commonly used. Table 2.3 summarizes important features of major nitrate removal methods used for drinking water application.

Table 2.3: Important features of some major nitrate removal technologies

S.N.	Nitrate removal technologies	Important features
1.	Adsorption	1. Requires saturated/spent adsorbent disposal. 2. pH and temperature effects are important. 3. Post treatment is often not required. 4. Removal efficiency varies with different adsorbent. 5. Medium operational cost.
2.	Biological methods	1. Requires biomass waste disposal. 2. Temperature effect is important. 3. Post-treatment is required due to microorganisms. 4. >99 % efficiency can be achieved. 5. Medium operational cost.
3.	Chemical methods	1. No waste disposal is required. 2. pH and temperature effects are important. 3. Post treatment is required due to production of byproducts. 4. Maximum reported efficiency >60-70%. 5. High operational cost.
4.	Ion exchange	1. Requires waste brine disposal. 2. pH and temperature effects are not important. 3. Post treatment is required due to corrosivity of product water. 4. Approx. 90 % efficiency can be achieved. 5. Medium operational cost.
5.	Reverse osmosis	1. Requires high TDS disposal 2. pH and temperature effects are not important. 3. Post treatment is required due to corrosivity of product water. 4. >95 % efficiency can be achieved. 5. High operational cost.

(Source: Bhatnagar and Sillanpaa, 2011)

Adsorption is generally considered to be a better water treatment method because of its convenience, ease of use, and simplicity of design. There are several factors that influence the selection of an appropriate adsorbent for removing nitrates from water.

(1) Initial concentrations of nitrate,

(2) Concentrations of other competing ions in water,

(3) Optimized dose of adsorbent,

(4) pH of water,

(5) Maintenance and operation.

Bhatnagar and Sillanpa (2011) compiled a list of several materials which have been examined as adsorbents for NO_3^- removal from water as shown in Figure 2.1.

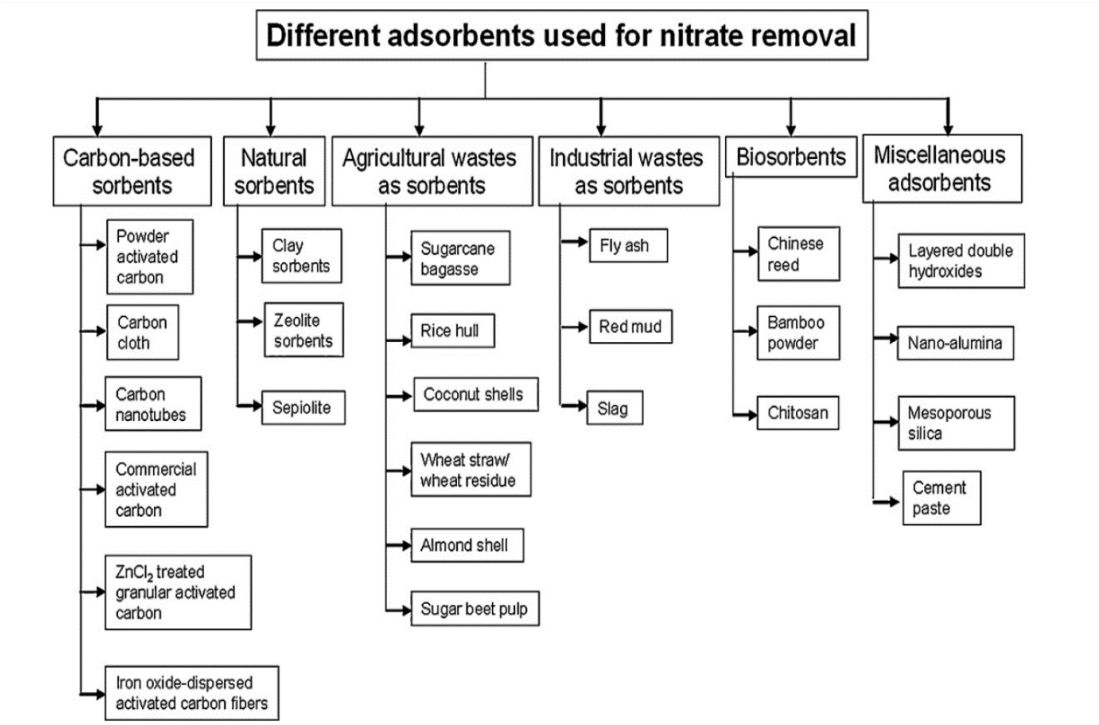

Figure 2.1: Different classes of adsorbents used for the removal of nitrate from water

Table 2.4 presents important characteristics of different adsorbents used for nitrate removal from water (Bhatnagar and Sillanpa, 2011).

Table 2.4 Important characteristics of different adsorbents examined for nitrate removal from water

S. N.	Adsorbent	Adsorbate adsorbed	Concentration range	Contact time	Temperature	pH	Reference
1.	Pure alkaline lignin	1.8 mmol/g	1-30 mg/L	2880 min	30°C	-	Orlando et al., 2002
2.	Sugarcane bagasse	1.41 mmol/g	1- 30 mg/L	2880 min	30°C	-	Orlando et al., 2002
3.	Pure cellulose	1.34 mmol/g	1-30 mg/L	2880 min	30°C	-	Orlando et al., 2002
4.	Rice hull	1.32 mmol/g	1- 30 mg/L	2880 min	30°C	-	Orlando et al., 2002
5.	Coconut shell activated carbon	2.66×10^{-1} mmol/g	-	-	30°C	2-4	Ohe et al., 2003
6.	Bamboo charcoal	1.04×10^{-1} mmol/g	-	-	30°C	2-4	Ohe et al., 2003
7.	Bamboo powder charcoal	1.25 mg/g	0-10 mg/L	7200 min	10°C	-	Mizuta et al., 2004
8.	Sepiolite activated by HCl	38.16 mg/g	100 mg/L	5 min	-	-	Öztürk and Bekta, 2004
9.	Unmodified sepiolite	408 mmol/kg	-	-	-	-	Özcan et al., 2005
10.	Surfactant-modified sepiolite	453 mmol/kg	-	-	-	2.0	Özcan et al., 2005
11.	Cross-linked and quaternized chinese reed	7.55 mg/g	10-40 mg/dm^3	10 min	25°C	5.8	Namasivayam and Höll, 2005
12.	Original & activated red mud	1.859 & 5.858 mmol/g	5-250 mg/L	60 min	25°C	6.0	Cengeloglu et al., 2006
13.	H_2SO_4 treated carbon cloth	2.03 mmol/g	115 mg/L	60 min	25°C	~7.0	Afkhami et al., 2007
14.	Raw wheat residue	0.02 mmol/g	50-500 mg/L	150 min	23 ± 2°C	6.8	Wang et al., 2007
15.	Modified wheat residue	2.08 mmol/g	50-500 mg/L	150 min	23 ± 2°C	6.8	Wang et al., 2007
16.	Ammonium-functionnalized mesostructured silica	46.0 mg/g	100-700 mg/L	60 min	5°C	<8.0	Hamoudi et al., 2007
17.	Powder activated carbon	10 mmol/g	-	60 min	25°C	<5.0	Khani and Mirzaei, 2008
18.	Carbon nanotubes	25 mmol/g	-	60 min	25°C	<5.0	Khani and Mirzaei, 2008

19.	Untreated coconut granular activated carbon	1.7 mg/g	5-200 mg/L	120 min	25˚C	5.5	Bhatnagar et al., 2008
20.	$ZnCl_2$ treated coconut granular activated carbon	10.2 mg/g	5-200 mg/L	120 min	25˚C	5.5	Bhatnagar et al., 2008
21.	Calcined hydrotalcite-type compounds	61.7-147.0 g/kg	12.7-236 mg/L	1440 min	25˚C	-	Socías-Viciana et al., 2008
22.	Layered double hydroxides	20-35 mg/g	0-1000 mg/L	240 min	21˚C	~8.5	Hosni and Srasra, 2008
23.	Impregnated almond shell activated carbon	16-17 mg/g	10-50 mg/L	120 min	20˚C	6.2	Rezaee et al., 2008
24.	Chitosan hydrobeads	92.1 mg/g	1-1000 mg/L	1440 min	30˚C	5.0	Chatterjee and Woo, 2009
25.	Chitosan beads	90.7 mg/g	25-1000 mg/L	24 ×60 min	30˚C	5.0	Chatterjee et al., 2009
26.	Conditioned cross-linked chitosan beads	104.0 mg/g	25-1000 mg/L	1440 min	30˚C	5.0	Chatterjee et al., 2009
27.	Wheat straw charcoal	1.10 mg/g	0-25 mg/L	10 min	15˚C	-	Mishra and Patel, 2009
28.	Mustard straw charcoal	1.30 mg/g	0-25 mg/L	10 min	15˚C	-	Mishra and Patel, 2009
29.	Commercial activated carbon	1.22 mg/g	0-25 mg/L	10 min	15˚C	-	Mishra and Patel, 2009
30.	Halloysite	0.54 mg/g	100 mg/L	1020 min	25˚C	5.4	Xi et al., 2010
31.	HDTMA modified QLD bentonite	12.83 - 14.76 mg/g	100 mg/L	1020 min	25˚C	5.4	Xi et al., 2010
32.	Chitosan coated zeolite	0.6-0.74 mmol/g	10-3100 mg/L	4320 min	4˚C and 20˚C	-	Arora et al., 2010
33.	Zr(IV)-loaded sugar beet pulp	63 mg/g	-	2440 min	15˚C	6.0	Hassan et al., 2010
34.	Chemically modified sugar beet bagasse	9.14 to 27.55 mg/g	10-200 mg/L	-	25-45˚C	6.58	Demiral and Gunduzoğlu, 2010

(Source: Bhatnagar and Sillanpa, 2011)

Subsequently, Ensie and Samad (2014) synthesized the SiO_2–FeOOH–Fe core shell and investigated its use in removing nitrates from water. At an initial concentration of 64 mg/L, a maximum nitrate removal of 99.84% was found at an optimal pH of 3 and a contact time of 2 h. The percentage removal depends heavily on the pH. As the initial nitrate concentration increases, the percentage removal increases. The sonication prevents the agglomeration of the nanostructure and leads to a more even distribution of the same, which ultimately leads to an increase in the percentage removal.

Jain et al. (2015) reported the impregnation of Mg, Fe, Co, Ni, Zn and Cu on aluminum oxide to improve nitrate sorption from aqueous solution. It was observed that the nitrate adsorption capacity was increased 13-fold using nickel-modified alumina compared to unmodified alumina, and the preference series of metals for impregnation on alumina was found to be Ni^{2+}> Co^{2+}> Zn^{2+}> Mg^{2+}> Cu^{2+}> Fe^{3+}. Adsorption experiments were carried out with an optimal dose of 2 g/L at 100 mg/L initial nitrate concentration for 6 h contact time. The Freundlich isotherm explained the adsorption process better than the Langmuir isotherm.

Chen et al. (2015) used bifunctional mesoporous silica to remove nitrate ions along with Pb. Maximum adsorption capacities of 712 µmol/g and 1120 µmol/g were found for Pb (II) and NO_3^- removal at pH 5.0.

Singh et al. (2015) carried out a series of experiments for removal of nitrates from aqueous solutions using hydrous bismuth oxides (HBO_3). HBO_3 shows a maximum nitrate sorption potential of 0.22 mg N^-/g with an initial nitrate concentration of 14 mg N^-/L. The absence of hydroxyl ions as exchange anion for nitrate removed

was indicated by the near neutral pH of the treated water. However, film diffusion and pore diffusion were found to play important roles in the sorption process. Furthermore, closer agreement with Boyd model confirmed that the rate-limiting process for the adsorption of nitrate ions on HBO_3 was by the external mass transfer.

Mehrabi et al. (2015) reported on the use of activated carbon and Fe_2O_3 nanoparticle composites to remove nitrate from water. The maximum removal of 91.3% was achieved with an adsorbent dose of 10.7 g/L in the pH range of 3-8. Based on the mean free adsorption energy E (kJ mol/L), the sorption process was found to be by physical adsorption.

Mahdavi et al. (2018) reported on humic acid-functionalized MgO, CeO_2 and ZnO nanoparticles (NPs) for removing nitrate from drinking water. The influence of various parameters such as pH (3– 8), temperature (15- 40°C), contact time (10- 1440 min) and liquid/solid weight ratio (L/S 525 mL/0.025 g) and initial nitrate concentration (22-220 mg/L) were studied. Metal oxide increased the removal efficiency of the adsorbent. The adsorption kinetics and isotherm data were found to correspond to the pseudo-second order and Freundlich models, suggesting the multilayer chemisorption of nitrate ions. The maximum adsorption capacities of nitrate ($N\text{-}NO_3^-$), calculated by endpoints of isotherm experiments were 86.4 mg/g for MgO, 57.6 mg/g for ZnO and 58.6 mg/g for CeO_2 respectively.

Ao et al. (2018) reported the use of Fe° / surfactant-modified activated carbon (AC) to remove nitrate from water. The adverse effect of increasing the pH on nitrate removal could be observed. At neutral pH a removal efficiency of 72.0% was reported

while at basic pH the nitrate removal decreased to about 58%. Kinetic studies showed faster removal under acidic pH conditions.

Ranjan et al. (2019) developed the hydrous bismuth oxide (HBO_2) supplemented with metals (Fe, Mg, Ca, Cu) for nitrate sorption from aqueous solution. Fe and Cu showed a good improvement in the nitrate sorption potentials compared to Mg and Ca. The nitrate uptake increased from 8.36 to 10.82 and 10.54 mg/g when iron or copper was added to the matrix of HBO_2 in comparison to unmodified HBO_2.

Fe-Mg-Mn-LDH was developed by coprecipitation methods and its adsorption properties for nitrate was investigated by Zhou et al. (2020) at an adsorbent dose of 5 g/L in real water. The main adsorption mechanisms of nitrate removal from aqueous solutions by Fe-Mg-Mn-LDH was found to be electrostatic attraction and ion exchange.

2.3 Technologies for fluoride removal from water

The traditional method of removing fluoride from drinking water uses lime. The precipitation and coagulation processes with iron (III), activated aluminum oxide, alum sludge and calcium have been extensively investigated. In developing countries like India, Kenya, Senegal and Tanzania, defluoridation of water has been done using the most popular technique called the Nalgonda technique. The process involves adding prescribed amounts of alum, lime, and bleach powder to the raw water, followed by rapid mixing, flocculation, sedimentation, filtration, and disinfection. After adding alum and lime to the raw water, insoluble flocs of aluminum hydroxide are formed, which settle on the bottom and co-precipitate fluoride. Bleaching powder ensures disinfection during the process of the Nalgonda technique. The entire process of the

Nalgonda technique for defluoridation has typically been used in a filling and drawing unit that is completed within 2-3 h. A series of batch operations in a 7-day cycle produces water sufficient for a small community (approx. 6200 people). However, treated water contains residual aluminum (ranging from 2 to 7 mg/L) which is higher than the established WHO standard of 0.2 mg/L (Bhatnagar et al., 2011). Ion exchange, reverse osmosis, and electrodialysis have also been suggested to remove excess fluoride from drinking water. Membrane processes have the disadvantage that they are relatively expensive to install and operate and are very susceptible to fouling, deposits or membrane degradation. In addition, the electrochemical techniques are expensive to install and maintain.

Ion exchange is one of the preferred methods of fluoride removal from water. Basic anion exchange resins containing quaternary ammonium functional groups are the most common exchangers for fluoride removal from water supplies. The chloride ion of the resin is replaced by the fluoride ion of the solution. The process continues until all active sites on the resin are occupied. The resin is regenerated using the supersaturated water with dissolved sodium chloride salt. Greater electronegativity of the fluoride ions is the driving force behind the replacement of chloride ions from the resin.

Adsorption is another commonly used method of removing fluoride from water. Various adsorbents were tried to find an efficient and economical defluorination system. Activated alumina is one of the most widely used adsorbents for fluoride removal from aqueous solutions. Hardness and surface loading (the ratio of the total fluoride concentration to the dose of activated alumina) are the two critical parameters

that affect the efficiency of fluoride removal by activated alumina. The adsorption process is completely pH-specific and delivers the best result in the pH range from 5.0 to 6.0. At pH> 7 silicate and hydroxide become stronger competitors of the fluoride ions for exchange sites and at pH <5 activated aluminum oxide becomes dissolved in an acidic environment, which leads to the loss of adsorbing media. Sarita Sansthan, Udaypur, Rajasthan used filters based on activated aluminum oxide with the support of UNICEF. It consisted of a bucket (approx. 20 L capacity) equipped with a microfilter that contained 5 kg of activated aluminum oxide at the bottom. This gives the best results of defluoridation (Meenakshi and Maheshwari, 2006).

Chubar et al. (2005) reported on the production of a new type of ion exchanger using iron (III) and aluminum double hydrous oxide ($Fe_2O_3 \cdot Al_2O_3 \cdot xH_2O$). It was used for the simultaneous adsorption of F^-, Cl^-, Br^-, and BrO_3^- from solutions. The process was found following a pseudo second order kinetics for fluoride and bromide sorption.

Maliyekkal et al. (2008) reported on magnesia amended activated alumina (MAAA) as a sorbent for the removal of fluoride from drinking water. MAAA was made by calcining alumina impregnated with magnesium hydroxide at 450°C. The amended sorbent produced showed a higher fluoride sorption potential from water than activated alumina. The influence of contact time, pH value, initial fluoride concentration and adsorbent dose was investigated in batch sorption experiments. To characterize the physicochemical properties of MAAA, X-ray diffraction (XRD), scanning electron microscope (SEM) and energy dispersive X-ray (EDAX) and gas adsorption porosimetry analyses were carried out. With an initial fluoride concentration of 10 mg/L, a removal efficiency of more than 95% was achieved within 3 h of contact

time at neutral pH. It has been found that the sorption of fluoride on MAAA is pH dependent and decreases at higher pH values. The kinetic data followed a pseudo second order model. A maximum sorption capacity of 10.12 mg/g fluoride was observed. Bicarbonate and sulfate in higher concentrations have been found to be a hindrance to fluoride sorption.

Biswas et al. (2009) synthesized ferric tin (IV) mixed oxide (HITMO) and used it to remove fluoride from water. The effects of pH, contact time and equilibrium parameters were studied with HITMO. The material was characterized by FTIR, XRD and SEM analyses. The morphology indicated a hydrated, amorphous and irregular surface of the mixed oxide. The kinetic data indicated a pseudo-second order reaction and the overall rate was found to be multistage one.

Sujana et al. (2009) performed a series of experiments to evaluate the effectiveness of amorphous mixed iron and aluminum hydroxides in removing fluoride from aqueous solutions. The adsorbent was produced by co-precipitating Fe and Al mixed salt solutions at pH 7.5 at room temperature. A wide range of Fe:Al molar ratios (1:0, 3:1, 2:1, 1:1, and 0:1) of the oxides were tested and the samples were characterized by XRD, BET surface area and pH_{PZC}. The amorphous nature of the adsorbent was indicated in the XRD result. pH, temperature, and initial fluoride concentration are the most influential parameters that affect fluoride removal in batch adsorption studies.

Sujana and Anand (2010) investigated fluoride removal using mixed hydroxides based on iron and aluminum in various molar concentrations. The maximum adsorption capacity for fluoride was given for Fe/Al with a molar ratio of 1:1. The adsorbent was

characterized before and after fluoride adsorption by XRD, TGA, SEM, EDX, TEM and FTIR analyses to understand the adsorption mechanism.

Ngameni et al. (2010) reported the use of charcoal impregnated with calcium compounds to remove fluoride. The materials were developed by impregnating wood with calcium chloride, followed by carbonization at 500°C, 650°C or 900°C. The charcoals were characterized by SEM, EDX, XRD and chemical titrations. The adsorbents were porous with a wood microstructure. XRD showed the presence of crystallized $CaCO_3$ and CaO. The pH of point of zero charge (pH_{PZC}) for charcoal was found to be in the range of 7.4 to 7.7.

Bhatnagar et al. (2011) has presented a summary of the properties of various adsorbents for fluoride removal from aqueous solutions (Table 2.5)

Table 2.5: Important characteristics of different adsorbents examined for fluoride removal from water

S.N.	Adsorbent	Adsorbate adsorbed	Concentration range	Contact time	Temperature	pH	Reference
1.	Alum sludge	5.394 mg/g	5-35 mg/L	240 min	32°C	6.0	Sujana et al., 1998
2.	Acid treated spent bleaching earth	7.752 mg/g	5-45 mg/dm^3	30 min	-	3.5	Mahramanlioglu et al., 2002
3.	Activated alumina (γ- Al_2O_3)	0.86 mmol/g	15-100 mg/L	384-1440 min	30°C	5.0-6.0	Ku and Chiou, 2002
4.	Hydroxyapatite Fluorspar Activated quartz Calcite Quartz	4.54 mg/g 1.79 mg/g 1.16 mg/g 0.39 mg/g 0.19 mg/g	2.50×10^{-5} to 6.34×10^{-2} mg/L	-	-	6.0	Fan et al., 2003
5.	Activated alumina (Grade OA-25)	1450 mg/kg	2.5-14 mg/L	-	-	7.0	Ghorai and Pant, 2004

6.	Metallurgical-grade alumina	12.57 mg/g	-	-	20°C	5.0-6.0	Pietrelli, 2005
7.	Alum-impregnated activated alumina	40.68 mg/g	1-35 mg/L	90 min	25°C	6.5	Tripathy et al., 2006
8.	Manganese-oxide-coated alumina	2.851 mg/g	2.5-30 mg/L	90 min	30 ± 2°C	7.0±0.2	Maliyekkal et al., 2006
9.	Aluminum hydroxide (THA & UHA)	23.7 mg/g & 7.0 mg/g	5.0-30 mg/L	1440 min	23 ± 2°C	7.0±0.3	Shimelis et al., 2006
10.	Quick lime	16.67 mg/g	10-50 mg/L	75 min	25 ± 2°C		Islam and Patel, 2007
11.	Magnesia-amended activated alumina	10.12 mg/g	5-150 mg/L	180 min	30 ± 1°C	6.5-7.0	Maliyekkal et al., 2008
12.	Schwertmannite	50.2-55.3 mg/g	10-90 mg/L	1440 min	30°C-22.6°C	3.8	Eskandarpour et al., 2008
13.	La (III) impregnated on Alumina	0.350 mM/g	2 mM/L	1200 min	25°C	5.7-8.0	Puri and Balani, 2009
14.	Hydrous-manganese Oxide coated alumina	7.09 mg/g	10-70 mg/L	120 min	25°C	5.2 ± 0.05	Teng et al., 2009
15.	Lime stone (LS) and Aluminum hydroxide impregnated lime stone (AlLS)	43.10 mg/g and 84.03 mg/g	100 mg/L	300 min	25°C	8.0	Jain and Jayaram, 2009
16.	Copper oxide coated alumina (COCA)	7.770 mg/g	10 mg/L	1440 min	30 ± 1°C	-	Bansiwal et al., 2010
17.	Calcium oxide-modified activated alumina and Manganese oxide modified activated alumina	101.01 mg/g and 10.18 mg/g	1-1000 mg/L	2880 min	25°C	5.5	Camacho et al., 2010
18.	Alkoxide origin alumina	2.0 mg/g	0-25 mg/L	1440 min	30 ± 2°C	7.0	Kamble et al., 2010
19.	Basic oxygen furnace slag	4.58-8.07 mg/g	1-50 mg/L	35 min	25-45°C	7.0	Islam and Patel, 2011

(Source: Bhatnagar et al., 2011)

Subsequently, Koilraj et al. (2013) used Zn-Cr-layered double hydroxides to remove fluoride from water. A maximum absorption capacity of 31 mg F^-/g was found in the batch experiment. Ion exchange has been inferred as the mechanism for fluoride uptake over a wide pH range (3-10) due to the buffering nature of LDH. Another modification of LDH with polysulfone resulted in high fluoride removal efficiency.

Tomar et al. (2013) performed a series of experiments to determine fluoride removal by Zr-Mn composite material. About 90% of the fluoride removal was achieved under optimal conditions of 24 g/L at pH 7 within a contact time of 2.41 min. The hydroxyl group of the adsorbent was a causative agent for the ion exchange of fluoride from the aqueous environment.

Chai et al. (2013) developed the sulfate-doped Fe_3O_4 / Al_2O_3 nanoparticles for fluoride removal from drinking water. Approximately 90% of the fluoride removal was recorded within 0.33 h of the reaction. The maximum Langmuir adsorption capacity was found to be 70.4 mg/g. However, different adsorption capacities were found at different initial concentrations. The observed displacement of sulfate by fluoride and the reduced sulfur content on the adsorbent surface indicated an anion exchange process as the dominant mechanism for fluoride adsorption by the sulfate-doped Fe_3O_4/Al_2O_3 nanoparticles.

Srivastav et al. (2013) investigated and found hydrous bismuth oxide (HBO_1) as a new material for defluorination from aqueous solution. The highest fluoride removal efficiency of 65% was observed with hydrous bismuth oxide (HBO_1) at an adsorbent dose of 50 g/L. The reaction was carried out for 3 h of contact time with

continuous stirring at ambient temperature (25±2°C). The pH of the treated water is observed in the range of 7.1-8.3, indicating that there is no hydroxyl ion involved in the adsorption to replace fluoride. The pseudo-second order kinetics and Langmuir isotherm appear to be a closer match than others, but the DR isotherm indicates the phenomenon of physical adsorption responsible for fluoride sorption.

He and Paul Chen (2014) used zirconium-based nanoparticles to treat excess fluoride from water. The maximum fluoride removal observed was 97.48 mg/g at pH 4 within 4 h of contact time. The ion exchange between sulfate and fluoride ions was indicated by FTIR and XPS analyses. Intra-particle surface diffusion was found to be the rate controlling step.

Dayananda et al. (2014) used CaO loaded mesoporous Al_2O_3 based adsorbents to remove fluoride from water. At a moderate adsorbent dose of 3 g/L, a removal of about 90% was achieved within 0.25 h, the maximum fluoride adsorption capacity being 136.99 mg/g. The kinetics of fluoride removal showed pseudo-second order and the adsorption followed the Langmuir isotherm. Chemisorption appeared to be the mechanism of fluoride adsorption.

Zhang et al. (2014) produced a mixture of La(III)-Al(III) loaded slag for fluoride removal from groundwater. The large amount of La-Al-O composite oxide existed on the surface of La-Al-Scoria, which is supposed to give excellent adsorption capacity for fluoride ions. The interaction between fluoride ions and the La-Al-O composite was explained by electrostatic attraction.

Habuda-Staniet al. (2014) published an excellent review on fluoride adsorption from aqueous solution. The results showed that metal oxides/hydroxides and their binary or trimetallic combination reflect the higher adsorption capacities for fluoride ions. Most frequently, however, oxides and hydroxides of titanium, iron and aluminum were tested and showed the highest adsorption capacities over the wide pH range.

Tomar et al. (2015) synthesized hydroxyapatite modified activated alumina (HMAA) for the removal of fluoride from contaminated drinking water. The hybrid adsorbent has a maximum adsorption capacity of 14.4 mg F^-/g, which is at least five times that of virgin activated alumina, which has been used extensively for fluoride removal.

Kameda et al. (2015 a) used the Mg-Al-layered double hydroxides intercalated with NO_3^- (NO_3•Mg–Al LDH) and Cl^- (Cl•Mg–Al LDH) to adsorb fluoride from aqueous solutions. Fluoride is removed from the solution by anion exchange, with NO_3^- and Cl^- being embedded in the LDH interlayer. The adsorption follows pseudo-second order reaction kinetics and the process follows Langmuir isotherm involving anion exchange. The maximum adsorption of 3.3 mmol/g on NO_3•Mg−Al LDH and 3.2 mmol/g on Cl•Mg−Al LDH were observed with equilibrium adsorption constant being 2.8 and 1.5 respectively.

Jin et al. (2015) found excellent fluoride removal using MgO microspheres. The maximum adsorption capacity was over 115.5 mg/g at pH 7, which followed the Freundlich isotherm model. The removal mechanism indicated was exchange of surface

carbonates from MgO adsorbed CO_2 molecules by fluoride. A novel hydroxyl and carbonate co-exchange mechanism was proposed for the first time.

Srivastav et al. (2015) reported about a new adsorbent, hydrous bismuth oxide (HBO_2) with fluoride sorption capacity. With an initial fluoride concentration of 10 mg/L and an adsorbent dosage of 100 g/L, the maximum fluoride removal efficiency was 51%. No involvement of hydroxyl ions was found as the pH of the treated water was measured around 7.3. The calculation of the mean adsorption energy (E) indicated physical adsorption as the predominant mechanism for fluoride removal.

Kameda et al. (2015 b) reported removal of fluoride using Mg-Al-layered double hydroxides intercalated with CO_3^{2-} (CO_3•Mg-Al LDH). The values of the maximum adsorption and the equilibrium adsorption constant were 3.0 mmol/g and 1.1 x 10^3, respectively, for Mg-Al oxide according to Langmuir's isotherm. The Fluoride in the F•Mg-Al LDH result of anionic exchanged in between F^- and CO_3^{2-} in solution. The adsorbent has been reported to have excellent removal efficiency after regeneration also. Therefore, Mg-Al oxide can be reused for fluoride removal.

Parashar et al. (2016) synthesized nanocomposites from polypyrrole/ hydrous tin oxide to remove fluoride from water. The monolayer adsorption capacity of 26.16-28.99 mg/g at pH 6.5± 0.1 was reported. A combination of ion exchange and adsorption has been reported as the mechanism of fluoride removal. The ion exchange between loosely bound chloride or hydroxyl ion of the adsorbent and negatively charged fluoride ions at pH> pHpzc has been considered as the dominant mechanism for fluoride sorption.

Chinnakoti et al. (2016) reported the use of trititanate nanotubes (TNT) to remove fluoride from water. The maximum fluoride adsorption capacity of 58 mg/g of the adsorbent was estimated, which is far better than that of the other reported nanomaterials. Hydrolysis leads to the formation of hydroxyl groups, which provide the active centers for fluoride sorption.

Cho et al. (2016) carried out sorption experiments of fluoride and lead on hydrous chitosan beads impregnated with zirconium oxide. A binary sorbate system was achieved that could be associated with an increased positive surface charge, which favors F^- adsorption compared to a single sorbate system. A pseudo-second order kinetics was observed. The Langmuir isotherm model showed maximum sorption capacities of 22.1 and 222.2 mg/g for fluoride and lead respectively.

Jin et al. (2016) used the MgO nanoplates to remove fluoride. The adsorption kinetics suggested a pseudo second order model. The adsorption process showed a Freundlich isotherm with an adsorption capacity of over 185.5 mg/g at pH 7. The exchange of hydroxyl and carbonates were reported to be the mechanism for fluoride removal.

Mudzielwana et al. (2017) carried out the defluorination with MnO_2-coated sodium bentonite for groundwater. More than 90% of fluoride removal was achieved by the Na-activated bentonite-clay ligand exchange at pH 4 with an initial F^- concentration of 5 mg/L and an optimal dosage of 1.5 mg/L.

Mukhopadhyay et al. (2017) synthesized cerium(IV) incorporated hydrous Fe (III) oxide (CIHFO) for fluoride removal from water. It was found that the fluoride

adsorption via CIHFO is an ion exchange process with hydroxyl ions following Freundlich isotherm. At an initial concentration of 15.0 mg/L, a fluoride adsorption capacity of 24.8 $\pm$ 0.5 mg/g at pH 5.0-7.0 was observed. The adsorbent was found to be effective in solutions with high concentrations of fluoride.

Tang et al. (2018) examined the hydroxyapatite decorated with carbon nanotube composite (CNT-HAP) for fluoride removal. Batch adsorption experiments were carried out to examine the defluorination capacity of CNT-HAP and found a maximum adsorption capacity of 11.05 mg/g for fluoride, and adsorption data fitted with Freundlich isotherm. In addition, the adsorption of fluoride follows a pseudo-second order kinetics. The adsorption capacity is strongly influenced by the pH and coexisting anions. The results of the characterization showed that the adsorption mechanism follows an anion exchange process.

Kameda et al. (2018) found magnesium oxide to be an effective adsorbent for fluoride due to the electrostatic attraction between the positively charged MgO and F^-. The calculated activation energy value indicated chemical adsorption and a maximum Langmuir adsorption capacity of 5.6 mmol/g was estimated.

Prathna et al. (2018) evaluated the iron oxide/aluminum oxide based nano adsorbents for the simultaneous removal of arsenic and fluoride from aqueous solutions. The nanocomposites followed the Langmuir isotherm and fit well with the pseudo-second order reaction kinetics for both arsenic and fluoride. The maximum sorption capacity of the nanocomposites for As(III), As(V) and F^- at pH 7 was 1136 µg/g, 2513 µg/g and 4 mg/g, respectively. The presence of F^- in the model water had a

synergistic effect on the removal of As(III) and As(V), while the presence of arsenic had no significant effect on the removal of F^- at pH 7.

He et al. (2019) prepared mesoporous aluminum oxide modified with lanthanum and cerium for the fluoride removal from aqueous solutions and the characterization of the adsorbents was done by XRD, BET, XRF, FTIR, TEM, XPS and pH_{PZC}. The optimized conditions showed the maximum adsorption capacity of 26.45 mg/g with a dosage of 2.0 g/L and an almost neutral state (pH = 6.0 ± 0.1). The interaction between metal and fluoride appeared leading to adsorption and presence of SO_4^{2-} and CO_3^{2-} present in the water was detrimental to the process.

Mondal and Purkait (2019) developed iron-aluminum nanocomposite and confirmed its efficiency in fluoride removal. The fluoride adsorption followed a pseudo-second order kinetic model, while the process was diffusion-controlled in several stages with the Langmuir isotherm being pursued. A maximum adsorption capacity of 42.95 mg/g was achieved with an adsorbent dosage of 0.25 g/L. Ion exchange could be the caustic mechanism for fluoride removal from solution.

Ogata et al. (2020) successfully synthesized magnesium and iron complex hydroxides (Mg-Fe-CH3.0 and Mg-Fe-CH5.0) and examined their ability to adsorb fluoride ions. Studies have shown that the adsorption mechanism is related to the ion exchange between fluoride ions and chloride ions in the interlayer space of the adsorbent. The author claims that the adsorbent has a high potential for adsorbing fluoride ions from the aqueous phase.

2.4 Technologies for arsenic removal from water

In order to help the social impact of arsenic challenges among the affected people, it is important to develop technologies to remove arsenic from drinking water. With adsorption considered to be the most common method of removing arsenic from water, various adsorbents have been developed (Mohan and Pittman, 2008). Activated carbon appears to be the most common adsorbent for arsenic adsorption (Gu et al., 2005; Chuang et al., 2005). Other adsorbents, such as activated alumina, ion exchange resins, sand, silica, clays, iron, iron compounds, and organic polymers (Mohan and Pittman, 2007) are as effective as activated carbon in removing arsenic. Activated aluminum oxide (Lin and Wu, 2001; Singh and Pant, 2004), sand coated with iron oxide (Thirunavukkarasu et al., 2002; Mohan and Pittman, 2007), granular iron hydroxide (Badruzzaman et al., 2004; Banerjee et al., 2008), modified activated aluminum oxide (Sarkar et al., 2008), hydrous iron oxide (Habuda-Stani et al., 2008), manganese oxide-coated aluminum oxide (Maliyekkal et al., 2009), activated carbon (Asadullah et al., 2014) zirconium oxide (Kwon et al., 2016), Mg / Al LDH (Rahman et al., 2016), zero-valent iron (Banerji and Chaudhari, 2017), iron-based granules (Hu et al., 2019), modified Fe_3O_4 nanocomposite (Dutta et al., 2020) and the application of nanomaterial oxides including iron, copper (Martinson and Reddy, 2009), silver, aluminum (Patra et al., 2012), titanium (Habuda-Stanic and Nujic., 2015), as adsorbents have been reported to show great promise (Lata and Samadder, 2016).

Based on the thematic reviews by McNeill and Edwards (1995) and Petrusevski et al. (2007), Feenstra et al. (2007) from the International Groundwater Resources Assessment Center, Netherlands, published “Arsenic in Groundwater: Review and

Evaluation of Removal Methods". Here, the arsenic removal methods were grouped as: (A) Common Methods and (B) Emerging Methods.

(A) Common methods are based on any of the four processes:

(i) Precipitation processes, including coagulation/filtration, direct filtration, coagulation assisted microfiltration, enhanced coagulation, lime softening, and enhanced lime softening,

(ii) Adsorptive processes, including adsorption onto activated alumina, activated carbon and iron/manganese oxide based or coated filter media,

(iii) Ion exchange processes, specifically anion exchange, and

(iv) Membrane processes, including nano-filtration, reverse osmosis and electrodialysis.

(B) Emerging methods includes:

(i) Fe-Mn-Oxidation

(ii) Green sand filtration

(iii) Coagulation assisted microfiltration

(iv) In situ (sub-surface) arsenic immobilization

(v) Enhanced coagulation (aka electro coagulation, electro flotation)

(vi) Biological arsenic removal

(vii) Phytoremediation

(viii) Electrokinetic treatment

(viii) Iron oxide coated sand (IOCS)

Additionally, there are (i) Memstill, (ii) Water Pyramid, and (iii) Solar Dew Collector.

A comprehensive list of adsorbents used in arsenic removal is given in Table 2.6.

Table 2.6: Important characteristics of different adsorbents examined for arsenic removal from water

S.N.	Adsorbent	Adsorbate adsorbed	Concentration range	Contact Time	Temperature	pH	References
1.	Iron(III)-loaded chelating resin	0.84 mmole/g As(III) 0.74 mmole/g As(V)	7.8-78 mg/L As(III) 0.79-7.9 mg/L As(V)	300 min	25˚C	8-10 2-4	Matsunaga et al., 1996
2.	Fe(III)/Cr(III) hydroxide	11.02 mg/g As(V)	10 mg/L As(V)	240 min	32˚C	3-10	Namasivayam and Senthilkumar, 1998
3.	Hydrous zirconium oxide	- As(III)/As(V)		-	25˚C	4–6	Suzuki et al., 2001
4.	Ferriginous manganese ore	72.58 % As(III) 72.16 % As(V)	0.12 mg/LAs(III) 0.19 mg/L As(V)	30 min	25˚C	2-8	Chakravarty et al., 2002
5.	Manganese dioxide	53 mg/g As(III)/ 22 mg/g As(V)	10-100 µg/L As(III)/ As(V)	120 min	<40˚C	-	Lenoble et al., 2004
6.	Activated alumina	96.2 % 0.180 mg/g As(III)	1 mg/L As(III)	360 min	25˚C	7.6	Singh and Pant, 2004
7.	Fe(III)-Si Binary Oxide	11.3-14.9 mg/g As(III) 21.1-21.5 mg/g As(V)	0.4-20 mg/L	24×60 min	20-21˚C	3 -9	Zeng L, 2004
8.	Titanium dioxide	32.4 mg/g As(III) 41.4 mg/g As(V)	0.4 - 80 mg/L	120-300 min	25˚C	8.5	Bang et al., 2005
9.	Iron oxide-coated sand	0.2 mg/L As(V)	0.5-2 µg/L As(V)	30-480 min	50˚C	4-10.2	Vaishya and Gupta, 2005
10.	Fe–Mn mineral material	8.5 mg/g As(III) 14.7 mg/g As(V)	100 µg/L - 100 mg/L	24×60 min	25±0.5˚C	3-7	Deschamps et al., 2005
11.	Iron hydroxide coated alumina	102 µmol/g As(III) 489 µmol/g As(V)	0.1–0.4 mmol/L As(III)/As(V)	48×60 min	20˚C	6.1± 0.3	Hlavay and Polyak, 2005
12.	Iron oxide-coated cement	As(III) As(V)	0.7-13.5 mg/L As(III) 0.5-10 mg/L As(V)	120 min	15-35˚C	7	Kundu and Gupta, 2006

13.	Hydrous Iron(III)-Tin(IV) Binary Mixed Oxide	43.86 mg/g As(III) 27.55 mg/g As(V)	5-20 mg/L	120 min	30˚C	3-9	Ghosh et al., 2006
14.	Hydrous stannic oxide	15.85 mg/g As(III) 4.3 mg/g As(V)	5-10 mg/L	180-240 min	27˚C	6.5–8.5	Manna and Ghosh, 2007
15.	Hydrous ferric oxide	85.3% As(III) < 100% As(V)	120 µg/L	240 min	40˚C	2-12	Jang and Dempsey, 2008
16.	Cupric oxide	26.9 mg/g As(III) 22.6 mg/g As(V)	0.1-100 mg/L	30 min	21-25˚C	6-10	Martinson and Reddy, 2009
17.	Iron(III)–titanium(IV) binary mixed oxide	85 mg/g As(III) 14.3 mg/g As(V)	5-10 mg/L	210 min	15-30˚C	7.0	Gupta and Ghosh, 2009
18.	Manganese oxide-coated-alumina	42.48 mg/g As(III)	2-300 mg/L	120-180 min	30˚C	4-10	Maliyekkal et al., 2009
19.	Magnetite (Fe_3O_4)	485 µg/g As(V)	100 µg/L	60 min	20-30˚C	8	Shipley et al., 2010
20.	Ce–Ti oxide adsorbent	6.8 mg/g As(III) 7.5 mg/g As(V)	20 µg/L - 20 mg/L	12×60 min	25˚C	4-10	Li et al., 2010
21.	Hydrous titanium dioxide	22.0–33.4 mg/g As(III) 25.8–32.1 mg/g As(V)	1.0 mg/L	240 min	20-23˚C	4-6	Pirilä et al., 2011
22.	Fe (III) -Cr(III) mixed oxide	55 mmole/g As(III)	0.10 - 0.13 mmol/L As(III)	120 min	30˚C	7	Basu and Ghosh, 2011
23.	Iron–zirconium binary oxide	46.1 mg/g As(III) 120.0 mg/g As(V)	5-20 mg/L	36×60 min	20-25˚C	7	Ren et al., 2011
24.	Iron oxide	1.2-20 mg/g As(III) 4.6-4.9 mg/g As(V)	0.3-100 mg/L	-	25˚C	6-9	Luther et al., 2012
25.	Hydrous cerium oxide	170 mg/g As(III) 107 mg/g As(V)	0.01-0.02 µg/L As(III) 0.01-0.02 µg/L As(V)	24×60 min	25˚C	6.8-7	Li et al., 2012
26.	Fe–Mn binary Oxide	114 mg/g As(III) 60 mg/g As(V)	5-40 mg/L	24×60 min	25˚C	7	Zhang et al., 2012
27.	Granular TiO_2	145-160 mg/g As(III)	0.39- 2460 mg/L	30 min	-	5-7	Yan et al., 2015
28.	Fe–Ni binary oxide	168.6 mg/g As(III) 90.1 mg/g As(V)	10 mg/L	-	25˚C	7 ± 0.1	Liu et al., 2015

Other than adsorption, Kumar and Goel (2010) reported the use of electrocoagulation to remove arsenic (and nitrate) from drinking water. The pollutant removal efficiency was determined by voltages in the range of 10-25 volts. The maximum removal efficiency was 84% for nitrate at 25 V and 75% for As(V) at 20 V.

Srivastava and Vaishya (2013) reported As(III) removal by dynamically modified iron-coated sand (DMICS). Coated sand particles easily adsorbed the arsenic and chemisorption was responsible for the sorption mechanism. The maximum Langmuir adsorption capacity of DMICS was calculated to be 0.29 mg/g. The sorption process was pH-dependent and the maximum arsenic removal took place in the pH range of 6-8.

Chen et al. (2013) performed a series of experiments to determine arsenic adsorption through Ce-Fe oxide coated multi-walled carbon nanotubes (CF-CNTs). Excellent arsenic adsorption were reported, and it was said that electrostatic attraction and surface complexation were the major mechanisms of As(III) and As(V) removal from water.

Zhang et al. (2013) used Fe (III) -Cu (II) binary oxide to remove arsenic from water. The maximum adsorption capacities of 82.7 and 122.3 mg/g for As(V) and As(III) were given at neutral pH. In addition, carbonate and sulfate do not affect arsenic removal, while phosphate reduces arsenic sorption at higher concentrations. The binary oxide was claimed to have inexpensive synthesis, easy regeneration, and excellent arsenic removing performance.

Han et al. (2013) prepared synthetic pyrite (FeS_2) for the adsorption of As(III) and As(V). The formation of strong inner-sphere complexes is the reason for the binding of arsenic to the pyrite. Therefore, pyrite could be treated as an effective adsorbent / reactant in removing arsenic under stable anoxic conditions.

Ghosh et al. (2014) produced Mn-incorporated Fe(III) oxide (MNFO) nanoparticles for use in removing arsenic as well as iron and phosphate from groundwater. For arsenic, the adsorption capacity per unit volume from column studies was recorded as 3.34 $mg/g/cm^3$. It is said to be a relatively inexpensive adsorbent of a harmless nature.

Habuda-Stanic et al. (2014) showed the possibilities of arsenic removal by pre-oxidation and its removal from the groundwater using iron coagulants. Arsenic was removed by Fe(III) ions in combination with potassium permanganate, whereas an iron-based coagulant with Fe(II) ions shows higher efficiency when hydrogen peroxide is used as an arsenic pre-oxidizer.

Habuda Stanic and Nujic (2015) reviewed this Application of nanoparticles and reported on various forms of TiO_2 or TiO_2-based materials for arsenic removal. It was found that an increase in the TiO_2 content increases the As(V) removal and the highest arsenic adsorption capacity is achieved by Fe_3O_4 magnetite nanoparticles at neutral pH (188.69 mg/g for As(III) and 153.8 mg/g for As(V)), while the lowest value for the impregnation of activated carbon granulate with Fe_2O_3 (0.181 mg/g for As(V) at pH 7 and room temperature).

Lata and Samaddar (2016) examined the use of nano adsorbents to remove arsenic from water and discussed various related challenges. Various transition metals such as Cu, Fe and Ti based compounds were investigated as arsenic removing adsorbents and their results were compared with other adsorbents. The author concluded that aluminum oxides and mixed metal oxide nanoparticles may be the best option for removing arsenic from wastewater and drinking water, respectively.

Pérez et al. (2016) investigated cationic polymer and hydrous zirconium oxide-based hybrid for As(III) and As(V) removal from water. With a higher hydrous zirconia content, higher As(III) sorption was reported, whereas a lower hydrous zirconia content showed greater As(V) sorption. The adsorption capacity of the adsorbent for As(III) and As(V) was found to be 18.8 mg/g and 19.1 mg/g, respectively. As(V) has a maximum adsorption in the pH range of 3.9- 4.5 due to the electrostatic interaction between arsenic species and adsorbent, while the maximum binding of As(III) due to the interaction between acid and base in the pH range of 7.5 to 8.0 drops.

Cantu et al. (2016) evaluated synthetic Fe_7S_8 nanoparticles for arsenic adsorption from water. Adsorption capacities of 14.3 mg/g and 31.3 mg/g were given for As(III) and As(V) adsorption. Adsorption was reported to be pH independent with low binding at pH 2 and high binding at pH 3 to about the first 20 minutes of contact time. The binding can take place through a combination of chemisorption and physisorption.

Chaudhry et al. (2016) performed a series of experiments using zirconia coated sand (ZrOCS) to remove arsenic from aqueous solution. The maximum adsorption capacity of the Langmuir monolayer was found to be 136.98 µg/g at 313 K. It was found that temperature and pH did not affect adsorption efficiency. Chemical bonds could have played an important role between As (III) and ZrOCS.

Rahman et al. (2016) developed Mg-Al layered double hydroxide (MgAl LDH), intercalated with NO_3^-, for As(V) adsorption from aqueous solutions. The adsorption process is well described by the Langmuir isotherm and the pseudo-second order kinetics. 142.86 and 76.92 mg/g are the maximum arsenic adsorption capacities for LDHs synthesized with initial Mg/Al molar ratios of 2 and 4, respectively. The chemisorption nature of adsorption and pseudo-second order kinetics was observed.

Kwon et al. (2016) synthesized composite adsorbent hydrous zirconium oxide on alginate beads (ZOAB) to remove As(III), As(V) and Cu(II) from the aqueous phase. The maximum sorption capacities for As(III), As(V) and Cu(II) were given as 32.3, 28.5 and 69.9 mg/g, respectively. In the presence of 48.6 mg/L Cu(II), the sorption capacity of As(V) increased from 1.5 to 3.8 mg/g after 240 h. The adsorption of As(III), As(V) and Cu(II) followed pseudo-second order kinetics with Freundlich and Langmuir isotherm models.

Prathna et al. (2017) evaluated the iron oxide nanoparticles for removing arsenic and fluoride. An effective fluoride removal efficiency was achieved with iron oxide nanoparticles at the pH values and concentrations investigated. Pseudo-first order reaction agrees with the adsorbent data and Freundlich isotherm model for As(III) and

As(V) (R^2 value of 0.93 and 0.98 at pH 7 respectively). The maximum sorption capacity was determined to be 909 and 3333 µg/g for As(III) and As(V) respectively. The results of the study indicated that the synthesized nanoparticles could be promising adsorbents for arsenic removal in small-scale water systems.

Kolomiyets et al. (2017) reported on the removal of As(V) with titanium oxyhydrate in the pH range of 3-10. In the alkaline state, a greater sorption capacity was observed than in the acidic state (pH range of 3-5). It was assumed that the influence of the negative charge the oxide surface increases arsenic adsorption.

Prathna et al. (2018) used iron oxide/alumina oxide nan composites to remove both fluoride and arsenic from aqueous solutions. The maximum sorption capacity was given as 1136 µg/g, 2513 µg/g and 4 mg/g for As(III), As(V) and F^- at pH 7, respectively. The results of the study indicated that the synthesized nanocomposites could be promising adsorbents for fluoride and arsenic removal in small water systems.

Zhang et al. (2019) developed Fe-Ti-Mn composite oxide (FTMO) for the efficient removal of arsenic from the water environment. The maximum adsorption capacities at 25°C were determined to be 74.4 mg/g for As(V) and 122.3 mg/g of As(III). Phosphates and silicates are the main anionic species that adversely affect arsenic removal efficiency. The author reported easy regeneration of adsorbent. The high adsorption capacities and the superior selectivity make the FTMO a promising candidate for the practical treatment of arsenic-contaminated water.

Kalaruban et al. (2019) used iron incorporated granular activated carbon (GAC-Fe) to remove As(V) from water. The author found a better arsenic removal efficiency

of GAC-Fe compared to unmodified GAC. The batch study confirmed that GAC-Fe had a higher Langmuir adsorption capacity at pH 6 (1.43 mg As (V)/g) than GAC (1.01 mg As(V)/g). The presence of heterogeneous adsorption sites was confirmed by adsorption experiments with intra particle diffusion in meso and micropores in GAC. Twice the volume of treated water could be achieved by GAC-Fe compared to unmodified GAC in a column study.

Hu et al. (2019) compared four treatment methods, namely ozonation-manganese-greensand filtration (OSF), OSF-iron-based granulate media adsorption (OSFIA), Burgess Iron Removal Method (BIRM) and BIRM-iron-based granulate media adsorption (BIA). on arsenic and manganese removal in Canada. The authors found that the OSFIA treatment gave the highest removal of arsenic and manganese.

Pantić et al. (2019) used copper-impregnated natural mineral tuff (T-Cu(A-C)) to remove arsenic. The high adsorption rate of pseudo-second order in the range of 0.5090.789 g/mg/min for As(V) and 0.3040.532 g/m/min for As(III) justified further use of T–Cu(A–C) in one Flow system. The fixed bed column adsorption data were fitted with empirical Bohart–Adams, Yoon–Nelson, Thomas, and Dose response models to indicate the capacities and breakthrough time dependence on influent arsenic concentration and flow rate.

Lingamdinne et al. (2019) used Graphene oxide-lanthanum fluoride nanocomposite for the adsorptive removal of arsenic from an aqueous environment. The maximum adsorption capacity was given as 18.52 mg/g (at 298 K) and was dependent on the pH value of the solution, the mass of the adsorbent, the contact time

and the As (V) concentration. The maximum adsorption capacity of 17.0 mg/g was observed. The pseudo second order kinetic model and Langmuir equation fit well with experimental data. The overall results suggest that adsorption occurs through complex formation on the inner surface and / or an ion exchange reaction, in particular above a neutral pH.

Pessoa Lopes et al. (2020) performed a series of experiments to remove As (V) from water using an integrated ion exchange membrane process in conjunction with Fe coprecipitation. The pH of the treated water was maintained within the recommended drinking water range of 6-9 without the need for external pH regulation and / or control.

Prabhakar and Samadder (2020) achieved an excellent result for As(V) removal from aqueous solutions using nano-alumina. The adsorption follows the Freundlich isotherm model. The maximum adsorption capacity of the monolayer was given as 1401.90 μg/g at an optimal temperature of 298 K. The kinetic data indicated that the film diffusion was the controlling step. Phosphate and sulfate significantly affect removal efficiency, while competing anions such as nitrate, bicarbonate, and chloride did not have a large impact on As(V) removal efficiency.

Dutta et al. (2020) developed Fe_3O_4 based nanocomposite as an effective adsorbent for removing arsenic from water. 98% removal efficiency of As(III) and As(V) correspond to 28.27 and 83.08 mg/g, respectively. As-Fe formation complexes via legend exchange was considered as the mechanism of arsenic removal.

Ranjan et al. (2021) reported removal of arsenic with Hydrous Bismuth Oxide (HBO1). The advantage of the adsorbent included simultaneous removal of arsenic and

fluoride from aqueous solution. Physical adsorption and ion exchange were observed as the mechanism of removal with an arsenic absorption potential of 13.1-19.6 μg/g at 0.08 mg/L As(V) concentration.

A review of the available literature indicates that the current available methods are often high in cost and the commercial technologies often require large centralized treatment units. In many cases, wells serve small communities which cannot be connected to centralized water treatment units. Therefore, it seems necessary to develop methods which are compact, transportable and easily manageable. Available technical data, experience and economies indicate that adsorption/ion exchange process is most suitable method for groundwater supply for its simplicity, effectiveness and relatively low cost.

2.5 Removal of nitrate, fluoride and arsenic in coexisting conditions

Several hydrous metal oxides (HMOs) have been used for removal of contaminants from drinking water. Obviously, some of the materials have been found useful for removal of more than one contaminant. Table 2.7 summarizes the results of some of such studies.

Table 2.7: Characteristics of adsorbents used for simultaneous removal of more than one contaminant (nitrate, fluoride and arsenic) coexisting in water

S. No	Adsorbents	Contaminants	Initial conc. (mg/L)	Efficiency/ Sorption Potential	Optimum pH range	Temp (°C)	Time (h)	Reference
1.	Polyacrylonitrile + Hydrazinehydrate	F^-, PO_3^{-4}, AsO_3^{-4} (Individual)	10 mg/L F^-	90.4% F^-	3.5 - 7.0	25	2	Ruixia et al., 2002
			30 mg/L PO_3^{-4}	99% PO_3^{-4}	3.0 - 5.5			
			38 mg/L AsO_3^{-4}	97.9% As(V)	3.0			

2.	Ce(IV)-doped iron oxide	As(V) + F^- (Simultaneous)	1.0 mg/L As(V) + 1.6 mg/L F^-	0.2 mmole/g As(V) + 0.9 mmole/g F^-	5-6	20	24	Zhang et al., 2003
3.	Aluminum sulfate octadecahydrate + Polymeric anionic flocculent	F^-, As(III)/As(V) (Individual)	5.9- 4.8 mg/L F^- 0.134-0.075 g/L As(III)/ As(V)	77% F^- 99% As(III)/ As(V)	7.1	-	3	Piñón-Miramontes et al., 2003
4.	Mg_4Al_2 LDH	F^-, As(V), NO_3^- (Individual)	10 mg/L F^- 16 mg/L As(V) 100 mg/L NO_3^-	80% F^- 100% As(V) 15% NO_3^-	7.78-8.5	-	7 5 7	Delorme et al., 2007
5.	Activated alumina	F^-, As(III)/As(V), NO_3^- (Individual)	50 µg/L As(III) 50 µg/L As(V) 10 mg/L F^- 50 mg/L NO_3^-	60-90% As(III) >90% As(V) 85-95% F^- 25-35% NO_3^-	5.5-8.3	-	-	Mahmood et al., 2007
6.	Cement paste	F^-+ PO_3^{-4} (Simultaneous) NO_3^-+ SO_4^{2-} (Simultaneous)	18.7 mM F^- + 19.5 mM PO_3^{-4} 5.06 mM NO_3^- + 19.5 mM SO_4^{2-}	1.67 meq/g F^- + 1.96 meq/g PO_3^{-4} 10.8 mg/g NO_3^- + 18.4 mg/g SO_4^{2-}	-	-	24	Park et al., 2008
7.	Hydrous ferric oxide	F^-+ As(V) + P (Simultaneous)	100 µg/L As(V)	86-98% F^- + 91-95% As(V) + 94-95% P	4–9	25 ±1	-	Streat et al., 2008
8.	Fe–Ce oxide	As(V) + F^- (Simultaneous)	13.3 mol/L As(V) + 13.3-1330 mol/L F^-	1.15 mmol/g As(V)	5.0±0.2	20	24	Zhang et al., 2010

9.	Nano-alumina	NO_3^-+ F^- (Simultaneous)	-	55% NO_3^-	4	25	1	Bhatnagar et al., 2010
10.	Alumina Calcium oxide	F^-+As(III)/As(V) (Simultaneous)	200µg/L As(III) + 5 mg/L F^-, 100µg/L As(V) + 5 mg/L F^-	90 µg/g As(III) + 300 mg/g F^-, 90 µg/g As(V) + 450 mg/g F^-	7-7.6	25	12	Li et al., 2011
11.	Mg-Al-CO_3	As(V) + F^- (Simultaneous) As(V) + NO_3^- (Simultaneous)	20 µg/L As(V) + 1 mg/L F^-, 20 µg/L As(V) + 5 mg/L NO_3^-	3516.2 µg/g As(V) 3479.3 µg/g As(V)	-	-	5×24	Dadwhal et al., 2011
12.	Polyaluminum chloride	As+ F^- (Simultaneous)	2 mg/L F^- + 200 µg/L As	50-55 % F^- + 75-85 % As	6.5-7.6	-	-	Ingallinella et al., 2011
13.	Iron and aluminum binary oxide	As(V)+ F^- (Simultaneous)	40 mg/L As(V) + 10 mg/L F^-	90% As(V) + 70% F^-	7.5	25 ± 1	4	Liu et al., 2012
14.	Titanium and lanthanum oxides impregnated on granular activated carbon (TLAC)	As(V)+ F^- (Simultaneous)	30 mg/L As(V) + 10 mg/L F^-	30.3 mg/g As(V) + 27.8 mg/g F^-	4−12	-	24	Jing et al., 2012
15.	Nickel hydrotalcite-like compound (NiAlHT) Magnesium hydrotalcite-like compound (MgAlHT)	F^-+As(V) (Simultaneous)	2 mg/L As(V) + 5 mg/L F^-	0.25 mg/g F^- (NiAlHT) 0.30 mg/g F^- (MgAlHT)	7.5±0.3	-	3.33	Jiménez-Núˇnez et al., 2012
16.	Activated alumina Activated carbon	F^-, NO_3^-, As(III) (Individual)	100 mg/L F^- 100 mg/L NO_3^- 50 µg/L As(III)	98 % NO_3^- 99 % F^- 96 % As(III) 94 % NO_3^- 90 % F^- 92 % As(III)	7.5± 0.2 7.0± 0.2	22.0 ± 2 22.0 ± 2	-	Abbas et al., 2014
17.	Mg-Al layered double hydroxides	As(V)+ F^- (Simultaneous)	200µg/L As(V) + 10 mg/L F^-	125.8 mg/g As(V) + 28.6 mg/g F^-	7.0 + 0.1	20-25	24	Huang et al., 2015
18.	Hydrated Cement Bricks Powder	As+ F^- (Simultaneous)	10 µg/L As + 5 mg/L F^-	1.92 mg/g As + 1.72 mg/g F^- 0.04 mg/g As +	2-9	25 ± 3	1.25	Bibi et al., 2015

	Marble Powder			0.84 mg/g F^- 0.02 mg/g As + 0.18 mg/g F^-				
19.	Hydrous bismuth oxide	NO_3^-+ F^- (Simultaneous)	60.2 mg/L NO_3^- + 4 mg/L F^-	9.48 mg/g NO_3^- + 0.54 mg/g F^-	7.3-7.9	25	3	Singh et al., 2015
20.	Acid-base treated laterite	As(III)+ F^- (Simultaneous)	500 µg/L As(III) + 10000 µg/L F^-	23.5 µg/g As(III) + 345 µg/g F^-	5	30	5	Rathore et al., 2016
21.	Nickel/polypyrrole (Ni/PPy 1:2)	As(III)+ F^- (Simultaneous)	100–1500 µg/L As(III) + 5–40 mg/L F^-	2.64 mg/g As(III) + 67.71 mg/g F^-	5–9	25	3	Srivastava et al., 2016
22.	TiO_2-La adsorbent	As(III)+ F^- (Simultaneous)	10 µg/L As(III) + 25 mg/L F^-	114 mg/g As(III) + 78.4 mg/g F^-	3–9	-	24	Yan et al., 2017
23.	Haix-Zr Haix-Fe-Zr	As(V)+As(III)+F^- (Simultaneous)	200 µg/L As(III) + 200 µg/L As(V) + 5 mg/L F^-	95.27% As(V) + 95.88% As(III) + 95.87% F^-	-	25	24	Phillips et al., 2018
24.	MgAlFe-LDH	As(V) + F^- (Simultaneous)	2 mg/L As(V) + 2 mg/L F^-	99.44% F^- + 99.8% As(V)	6	25	24	Hongtao et al., 2018

Some of the finer details of these studies are as follows:

Zhang et al. (2003) reported co-adsorption of As(V) and F^- using a new Ce–Fe adsorbent. The surface of Ce–Fe adsorbent was considered positive at pH<5.8 as pHpzc of the adsorbent is found 5.8. Hence, As(V) and F^- removal was considered possible at pH> 5.8 and ion exchange with surface hydroxyl groups as mechanism. The adsorption pattern of As(V) fitted well with pseudo-first-order rate equation and both Langmuir and Freundlich models appeared applicable for sorption.

Delorme et al. (2007) examined the removal of F^{-}, As (V), and NO_3^{-} from water individually using calcined quintinite (Mg_4Al_2 double layer oxide). The adsorbent was found to have good affinity for F^{-} and As (V) but lower uptakes of NO_3^{-} due to competition with OH^{-}. Presence of CO_3^{2-} was found as strong competing anion for F^{-} and NO_3^{-}.

Streat et al. (2008) reported on the adsorption of arsenic, phosphorus, fluoride and cadmium ions using granular iron hydroxide. The effect of the presence of fluoride on arsenic removal was studied. The isoelectric point (IEP) of the adsorbent was found to be in the range of 7-8 and the adsorption of cadmium indicated an amphoteric nature of the material.

Zhang et al. (2010) examined the effect of competing F^{-} and phosphate ions on As(V) removal from water by Fe–Ce oxide. It was found that As(V) and phosphate are adsorbed primarily to the surface hydroxyl group attached to the Fe surface active sites whereas the fluoride are adsorbed to the Ce surface active sites. Active surface inhibited the two categories of binding sites. Phosphorous strongly inhibited the adsorption of arsenate at the low-binding-energy sites whereas fluoride got attracted towards high-binding-energy sites. The low-energy surface site, at which As(V) is loosely bound, has a higher maximum absorption capacity (Q_1= 1.05 mmol/g), while the high-energy site, at which As(V) is relatively tightly bound, has a smaller maximum absorption capacity (Q_2= 0.80 mmol/g) through Langmuir two-site equations.

Li et al. (2011) reported the use of highly ordered mesoporous alumina and calcium-doped alumina for F^{-} and arsenic removal from water. The materials exhibited strong affinity to F^{-} and the highest defluoridation capacity as 450 mg/g. They also

showed very high arsenic removal ability. Mesoporous alumina was able to remove 200 L of arsenic contaminated water per gram of material with a pH value of 7, reducing the concentration of As(V) from 100 ppb to 1 ppb.

Dadwhal et al. (2011) used Mg-Al double layered hydroxide as adsorbent for removal of arsenic in the presence of F^- from water. Experiments were done to assess the arsenic removal efficiency in the presence of competing anions in the range from 1:1 to 1:32. The adsorption of arsenic in the presence of these competing ions on LDH followed the extended Sips isotherm. The study concluded that of among those ions, fluorides and nitrates have the least effect on arsenic adsorption followed by chlorides, carbonates, sulfates, and phosphates. Phosphates, in particular, have a very strong impact.

Ingallinella et al. (2011) studied the simultaneous removal of arsenic and fluoride from groundwater by coagulation-adsorption using poly aluminum chloride in batch and continuous mode of experiment. Removal efficiency of 75-85% of arsenic and 50-55% of fluoride were achieved with influent concentration of 90 to 70 μg/L and 2.8 to 3.1 mg/L of F^- respectively.

Liu et al. (2012) used the iron and aluminum binary oxide ($FeAlO_xH_y$) to achieve the simultaneous removal of As(V) and F^-. The introduction of aluminum oxyhydroxide (AlO_xH_y) to iron oxyhydroxide (FeO_xH_y) within iron and aluminum binary oxide ($FeAlO_xH_y$) enables the removal of F^- as well as As(V). AlO_xH_y may simultaneously remove As(V) and F^- over a wide pH range from 4 to 11. $FeAlO_xH_y$ may be coated onto porous carriers such as diatomite to develop a novel adsorbent to treat water with simultaneously present As and F^-.

Jing et al. (2012) applied titanium and lanthanum oxides impregnated on granular activated carbon (TLAC) to achieved simultaneous adsorption of arsenate and fluoride. The Ti-As bond was found to give the evidence of arsenic attachment with Ti whereas fluoride was adsorbed on lanthanum oxides. Adsorption capacities of 30.3 mg/g of As(V) and 27.8 mg/g of F^- on TLAC was reported. The results of this study indicate that TLAC could be used as an effective adsorbent for simultaneous removal of As(V) and F^-.

Jimnez-Nnez et al. (2012) reported on the removal of fluorides in the presence of arsenic by compounds similar to nickel and magnesium hydrotalcite (NiAlHT, MgAlHT). It was observed that Elovich's kinetic model and chemisorptions of F^- dominated the process. It was found that the interferences of the competing anion in fluoride adsorption follow the order SO_4^{2-}> As(V) > Cl^-.

Huang et al. (2015) found the simultaneous removal of arsenic and fluoride ions by MgAl-layered double hydroxides with chloride and carbonate ions as interlayer anions in water. Arsenate sorption was the result of an ion exchange mechanism with chloride and carbonate, while fluoride sorption resulted only from chloride ion exchange. The adsorbent showed excellent adsorption properties for As(V) and F^- with maximum capacities of 125.8 and 28.6 mg/g, respectively, under neutral conditions.

Bibi et al. (2015) used hydrated cement as adsorbent for simultaneous removal of arsenic and fluoride from water. Maximum 97% and 80% removal of arsenic and fluoride respectively was reported. Adsorption reaction follows the Langmuir isotherm giving 1.92 mg/g and 1.72 mg/g for arsenic and fluoride removals respectively.

Singh et al. (2015) reported on the use of a mixed hydrous bismuth oxide (HBO_1+HBO_2) for the simultaneous removal of nitrate and fluoride from aqueous solutions. Bicarbonates and sulfates are the competing anions in groundwater, which significantly reduce performance and therefore require pre-treatment through the use of the media for drinking water treatment. The Weber-Morris model suggests that film diffusion and pore diffusion both play an important role in the sorption process, while the Boyd model confirms that external mass transport mainly determines the rate-limiting process for adsorption.

Srivastava et al. (2016) used Ni/Polypyrrole (PPy) nanocomposite as adsorbent for removal of arsenic and fluoride from contaminated water. The Ni/PPy nanocomposite prepared in the ratio of 1:2 acts as efficient adsorbent with maximum sorption potential of 2.64 and 67.71 mg/g of arsenic and fluoride respectively. Adsorbent reflect relatively higher preference for fluoride with respect to arsenic. The zero point charge of the nanocomposite in acidic pH suggests that the positive surface charge of adsorbent in acidic pH attracts the F^- and As(III) ion electrostatically and facilitates its removal.

Yan et al. (2017) examined the granular composite material TiO_2-La for the simultaneous removal of arsenic and fluoride. The material showed high adsorption capacities for As(III) (114 mg/g) and F^- (78.4 mg/g) in the pH range from 3 to 9, resulting in a high percentage (> 90%) of As(III) and fluoride adsorption have been achieved. Co-adsorption experiments showed that high fluoride concentrations inhibit As(III) adsorption, while the As(III) present at the same time has no significant influence on fluoride removal. The mechanisms at the molecular level showed that As (III) adsorption is only favorable at Ti sites at pH <7, while La adsorption sites can also

be occupied by As-La at pH> 10. The F^- adsorption is pH dependent and took place mainly at La sites. The granular TiO_2-La with high As(III) and fluoride adsorption capacity can be used to remove As(III) and fluoride at the same time. The findings from this study shed new light on the interaction mechanism of As(III) and F^- with the TiO_2-La composite.

Hongtao et al. (2018) described the synchronous adsorption of As(V) and F^- from aqueous solutions on MgAlFe-LDHs with different intercalating anions. F^- ion had advantages in the competitive adsorption on MgAlFe–Cl^- LDH and MgAlFe–NO_3^- LDH while MgAlFe–NO_3^- LDH for the adsorption of As(V) and F^- in coexisting systems with a concentration of each pollutant of 2 mg/L and an adsorbent dosage of 1.5 g/L. During the simultaneous removal process from a mixed system, As(V) and F^- compete for adsorption sites on the material and the results indicated that F^- is more in competition with MgAlFe–Cl^- LDH and MgAlFe–NO_3^- LDH. Strong interaction between As(V) and F^- and surface composition of the adsorbent make the adsorbent more efficient in removing arsenic and fluoride at the same time.

2.6 Selection of adsorbent

A review of available literatures suggests that among the various metal oxides used for anionic contamination removal, very few metal oxides have been explored for simultaneous removal of anionic contaminants i.e., nitrate, fluoride and arsenic from aqueous solution. In the recent years, bismuth has attracted considerable interest as potential sorbent. First, Fritsche (1993) reported removal of nitrate and other anionic contaminants by yellow bismuth hydroxide. Further, fluoride removal was reported (Srivastav et al., 2013; Singh et al., 2015; Ranjan et al., 2015). Hence, it's

imperative to examine hydrous bismuth oxides for potential use in simultaneous removal of nitrate, fluoride and arsenic from water for drinking purpose.

2.6.1 Hydrous bismuth oxides (HBOs) in nitrate, fluoride and arsenic removal from water

Bismuth is a silvery white metallic element in group V of periodic table with nitrogen, phosphorus, arsenic, and antimony above it. The metallic properties of bismuth are more pronounced than that of either arsenic or antimony (Bhakti, 1977). As an element, bismuth is one of the least toxic heavy metal and cases of bismuth poisoning in industrial use have not been reported till date (Reda et al., 2021). The field of application of bismuth based chemicals is very broad and extends from the pharmaceutical industry via the substitution of toxic lead compounds to the electronics industry, where bismuth compounds are frequently used because of their unique properties. Therefore, toxicity is not a problem in handling of bismuth (Howe, 1968; Udalova et al., 2008; Cheng and Zhang, 2018).

Krause and Nelson (1956) used the "mixed oxides of bismuth" and found high selectivity for chloride ion in natural solutions. In 1960, the United Kingdom Atomic Energy Authority patented a method for recovery of plutonium (as anionic complex) from uranium and/or fission products using bismuth hydroxides. Ito and Yashida (1970) used bismuth hydroxide, $Bi(OH)_3$ for the adsorption of chloride. In a study, Anand and Baxi (1978 a,b) reported removal of various anions such as Cl^-, Br^-, I^-, SO_4^{2-}, HPO_4^{3-}, PO_4^{3-}, and CrO_7^{2-} from sodium salt by bismuth nitrate and basic bismuth silicate using the ion exchange process. Fritsche (1993) reported removal of nitrate using yellow bismuth hydroxide precipitate. Mishra and Singh (1998) used hydrous bismuth oxide for adsorption of barium ion at micron level and reported the process to be favored at

higher concentration, higher temperature and pH. The reaction was found to follow first order rate law and obey Freundlich isotherm with irreversible nature of adsorption.

Singh (1999) observed that among various solid bismuth compounds such as bismuth oxide, bismuth oxychloride, bismuth carbonate and bismuth hydroxide, only bismuth hydroxide showed some adsorptive properties for nitrate from aqueous solutions. Bismuth hydroxide is observed as white color fine powder in its monomeric form. However, the method of preparation of bismuth hydroxide has significant effect on the physico-chemical properties of the material and their adsorptive properties (Singh and Ghosh, 2000). The performance and efficiency of hydrous bismuth oxides (HBOs), synthesized through precipitation in presence of excessive hydroxide, was investigated for nitrate removal from water. Yellow bismuth hydroxide is possibly the polymeric form of hydrous bismuth oxide(s) and shows significant nitrate sorptive properties (Singh et al., 2012). Srivastava et al. (2013) synthesized one form of hydrous bismuth oxide, designated as HBO1 and examined fluoride removal using it. A fluoride removal efficiency of over 60% was reported at a dosage of 50 g/L HBO1 in 3 h contact time. Liu et al. (2016) synthesized bismuth oxide ($Bi_2O_{2.33}$) by facile solvothermal method and found gainful sorption with maximum adsorption capacities up to 285 and 229 mg/g for I^- and IO_3^- over wide range of pH. The selectivity towards iodine is attributed due to the adsorption-induced chemical reaction as well as the micro/nanostructure of the flower-like $Bi_2O_{2.33}$ particles. In a similar attempt for applicability, Zhang et al. (2017) prepared a bismuth oxide/layered double hydroxide composites and tested for removal of excess iodine from water. The maximum iodine sorption capacity of 101.9 mg/g was reported at a neutral pH. The Langmuir isotherms and pseudo-second-order kinetic model was found better describing the iodine

adsorption onto the Bi_2O_3/LDHs composites. Zhu et al. (2018) prepared bismuth-impregnated aluminum oxide and used it as scavenger for arsenic from water. Uptake of arsenic followed chemisorption and 91.6% of removal efficiency was obtained at an initial As(III) concentration of 5 mg/ L with flow rate of 1 mL/ min.

Various adsorbents based on bismuth and their preparatory methods for the removal of targeted ions from water have been summarized in Table 2.8.

Table 2.8: Characteristics of hydrous bismuth oxides (HBOs) and their preparation methods for nitrate, fluoride and arsenic removal from water

S. N.	Bismuth compounds or HBOs	Ions removed	Preparation method	Reference
1.	Yellow bismuth hydroxide	PO_4^{3-}, NO_3^-, SO_4^{2-}, Cl^-	0.1M Bi_2O_3 in 2N HCl + 2N NaOH (1:3 V/V)	Fritsche, 1993
2.	Yellow hydrous bismuth oxide (HBO_2 & HBO_3)	NO_3^-	0.1M Bi_2O_3 in 2N HCl + 2N NaOH (1:2 and 1:3 V/V)	Singh and Ghosh, 2000
3.	White hydrous bismuth oxide (HBO_1)	F^-	0.1M Bi_2O_3 in 2N HCl + 2N NaOH (1:1 V/V)	Srivastav et al., 2013
4.	Bismuth oxide ($Bi_2O_{2.33}$)	I^-	Bismuth nitrate penta hydrate + Ethanol and Ethylene glycol (2:1 V/V)	Liu et al., 2016
5.	Bi_2O_3/LDHs composites	I^-	Bismuth nitrate penta hydrate + Ethanol and Ethylene glycol	Zhang et al., 2017
6.	Bismuth-impregnated aluminum oxide	As(III)	$Bi(NO_3)_3$ + HCl+Al_2O_3	Zhu et al., 2018

(Source: Ranjan et al., 2020)

2.7 Summary of Literature Review and Objectives of the present study

With an ultimate objective of developing an inorganic sorptive material to remove nitrate, fluoride and arsenic simultaneously from water, the literature review focused on collecting relevant information from the use of inorganic materials in such applications. It is observed that nitrate, fluoride and arsenic removal from groundwater intended for drinking have attracted significant attention of scientific community across the world and several metal oxides, hydroxides, bi metal oxides or layered double hydroxides (LDH) have been examined for their possible application towards such purposes. However, there is practically no report available on simultaneous removal of all the three contaminants coexisting together.

The present study also reviewed some significant developments in the area of use of hydrous bismuth oxides (HBOs) in water quality improvements. Based on such analyses, it is considered appropriate to examine HBOs in detail and evaluate their anionic sorptive properties towards simultaneous removal of nitrate, fluoride and arsenic coexisting in groundwater with levels as reported from different parts of the country.

2.8 Characterization techniques of selected inorganic adsorbent (HBO)

As for the characterization of HBO, research efforts focused on surface morphology, elemental analysis, functional group and the pH of point of zero charge (pHpzc). Some important and common techniques used in characterization of adsorbents are summarized in Table 2.9.

Table 2.9: Techniques for characterization of inorganic adsorbents

S.N.	Characteristics	Techniques
1.	Crystal structure	X-ray diffraction (XRD)
2.	Morphology	Scanning Electron Microscope (SEM)
3.	Elemental analysis	Energy-dispersive X-ray spectroscopy (EDS)
4.	Functional group on surface	Fourier Transform Infra-red spectroscopy (FTIR)
5.	pH_{PZC} (Point of Zero Charge)	Fast alkalimetric method

2.9 Research aim

In the present study, hydrous bismuth oxide has been investigated with the aim to evaluate the simultaneous removal of nitrate, fluoride and arsenic from water.

Both forms of arsenic were tested and it was found that removal for arsenate was higher than arsenite. Hence, arsenate was chosen for further experiments.

2.10 Scope of the present study

The available reports on groundwater quality in India show that there are several districts where all the three major contaminants, namely nitrate, fluoride and arsenic are present in concentrations beyond the limits for drinking.

Although numerous studies have been undertaken to treat groundwater to remove individual contaminants, such as nitrate, fluoride, or arsenic using hydrous metal oxides, there is very little information available on simultaneous removal under coexisting conditions. A few studies have reported removal of two contaminants, but simultaneous removal of all the three contaminants have not been examined.

Given the observed potentials of hydrous bismuth oxides (HBOs) for the removal of anionic pollutants through adsorption, the present study focused on investigating the use of HBOs to simultaneously remove all three pollutants, namely nitrate, fluoride and arsenic, which are commonly reported to exist in groundwater for drinking purposes.

With an ultimate objective of developing bismuth based inorganic sorptive media for simultaneous removal of nitrate, fluoride and arsenic from water for drinking purpose, the scope of the present study was defined as follows:

1. To check the possibility of using hydrous bismuth oxides (HBOs) for simultaneous removal of nitrate, fluoride and arsenic from water.

2. To estimate the nitrate, fluoride and arsenic removal potentials of selected hydrous bismuth oxides.

3. Characterization of the selected materials by XRD, SEM, EDS, FTIR and pH_{pzc} analyses to understand the process governing their removal.

4. To study their regeneration and reuse potentials for multiple cycle applications.

5. To study the effect of competitive anions, such as bicarbonate and sulfate on the contaminants removal potentials of the selected material

6. To examine their use in actual groundwater conditions spiked with reported levels of contamination by nitrate, fluoride and arsenic to make them suitable for drinking.

7. To record the lessons learnt and way forward.